

A Hybrid Approach to Model the Temperature Effect in Tire Forces and Moments

Bibin S

A Thesis Submitted to
Indian Institute of Technology Hyderabad
In Partial Fulfillment of the Requirements for
The Degree of Master of Technology

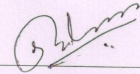


Department of Mechanical and Aerospace Engineering
Indian Institute of Technology Hyderabad

July 2015

Declaration

I declare that this written submission represents my ideas in my own words, and where ideas or words of others have been included, I have adequately cited and referenced the original sources. I also declare that I have adhered to all principles of academic honesty and integrity and have not misrepresented or fabricated or falsified any idea/data/fact/source in my submission. I understand that any violation of the above will be a cause for disciplinary action by the Institute and can also evoke penal action from the sources that have thus not been properly cited, or from whom proper permission has not been taken when needed.



(Signature)

Bibin S

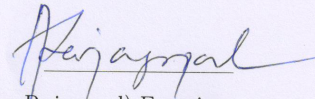
(Bibin S)

ME13M1004

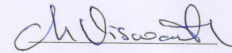
(Roll No.)

Approval Sheet

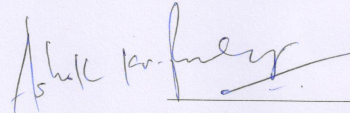
This Thesis entitled A Hybrid Approach to Model the Temperature Effect in Tire Forces and Moments by Bibin S is approved for the degree of Master of Technology from IIT Hyderabad



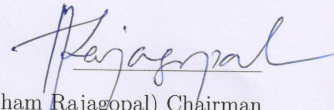
(Dr. Amirtham Rajagopal) Examiner
Civil Engineering, IITH



(Dr. Viswanath Chinthapenta) Examiner
Mechanical and Aerospace Engineering, IITH



(Dr. Askok Kumar Pandey) Adviser
Mechanical and Aerospace Engineering, IITH



(Dr. Amirtham Rajagopal) Chairman
Civil Engineering, IITH

Acknowledgements

I am thankful to all the people who have guided and supported me throughout my thesis work. First of all, I express my immense gratitude to my advisor Dr. Ashok Kumar Pandey, for giving me a chance to work in such an interesting field and believing in me during the research work. I also thank him for his excellent guidance and all time valuable support and encouragement.

I would like to extend my gratitude to my committee members who have made interesting and useful remarks during my thesis work. I also wish to thank Professor V. Eswaran, H.O.D, Department of Mechanical and Aerospace Engineering, IIT Hyderabad and Professor U.B Desai, Director, IIT Hyderabad for their support in various ways. I acknowledge all the faculty members of Mechanical Engg. Dept., IIT Hyderabad, specially Dr. Viswanath Chinthapenta, Dr. Chandrika Prakash Vyasarayani, Dr. M. Ramji, Dr. B. Venkatesham, Dr. R. Prasanth Kumar, being a student of whom during the course work, I got the opportunity to learn many new techniques as well as concepts which were directly or indirectly useful in my thesis work. I would also like to thank all staff members, project associate staffs, research scholars and MTech colleagues in CAE Lab, Department of Mechanical and Aerospace Engineering, IIT Hyderabad, for their help and suggestions, whenever needed. I must not ignore the special contributions of the institute library for providing all the necessary books, articles, and access to many useful domains to enrich my asset list in this research work.

Many, many thanks go to my family for their blessings and support. I wish to express my special gratitude to my lovable mother Lohitha V and my caring father S. Sasidharan for their care and love and to my younger brothers, Bijith and Vaishnav, and my sister, Vishnupriya, for giving me the base support through out this period. I am also thankful to my IIT Hyderabad friends for the warmth of their friendship and providing a supportive environment, which has made my stay at IIT Hyderabad wonderful. I sincerely acknowledge some of my close friends Mekha Vimal, Krishnadas, Jofin, Vinu, Sriram, Joseph, Tejus, Hari, and others for their role as tension healers and as rich sources of entertainment.

Dedication

Dedicated To

My Beloved Parents
(Mr.Sasidharan S and Mrs. Lohitha .V)

Abstract

Tire is an integral part of any vehicle, providing contact between the vehicle and the surface on which it moves. Forces and moments generated at the tire-road interaction imparts stability and control of motion to the vehicle. These forces and moments are functions of many variables such as slip, slip angle, contact pressure, inflation pressure, coefficient of friction, temperature, etc. This thesis deals with the effect of temperature on the lateral force, the longitudinal force and the self-aligning moment. The analysis is done at different tire surface temperatures (20°C, 40°C, 60°C). Since the experimental set up with the tire mounted is complex and expensive, we use a hybrid approach in which we take the results from the experiments done by the researchers on a sample piece of tire rubber at various temperatures. Then, we do the steady state analysis in ABAQUS considering the variation of coefficient of friction, slip speed and the elastic modulus of rubber with temperature. The steady state numerical results from ABAQUS at different surface temperatures are compared with the modified magic formula, i.e., PAC2002 tire model, to capture the temperature effect. After validating the variations of steady state forces and moments from ABAQUS with the modified PAC2002, we use these steady state tire models to do the transient analysis in order to capture the effect of temperature on the transient response of tire forces and moments for different driving conditions of acceleration, braking and double lane change using MSC ADAMS/CAR.

Contents

Declaration	ii
Acknowledgements	iv
Abstract	vi
Nomenclature	viii
1 Introduction	1
1.1 Tire Structure	2
1.1.1 Types of Tire based on Tire Structure	2
1.1.2 Tire Markings	4
1.2 Tire Forces and Moments	4
1.2.1 Longitudinal Force	6
1.2.2 Lateral Force	7
1.2.3 Self Aligning Moment	7
1.3 Tire Models	8
1.3.1 Brush Model	8
1.3.2 Ftire Model	9
1.4 Literature Review	9
1.5 Outline of the Thesis	12
2 The Magic Formula PAC2002 Tire Model with Temperature effects	13
2.1 Lateral Force at Pure Slip	14
2.2 Longitudinal Force at Pure Slip	16
2.3 Self Aligning Moment at Pure Slip	19

2.4	Summary	21
3	Steady State Analysis - FEM Approach	22
3.1	FEM Modeling	22
3.2	Steady State Rolling Analysis	24
3.2.1	Steady State Lateral Force	24
3.2.2	Steady State Longitudinal Force	26
3.2.3	Steady State Self Aligning Moment	27
3.3	Summary	28
4	Transient Analysis with the effect of Temperature	31
4.1	ADAMS Transient Model:	31
4.1.1	Cornering Analysis	34
4.1.2	Acceleration and Braking Analysis	36
4.2	Summary	38
5	Conclusion and Future Work	39

Chapter 1

Introduction

A vehicle tire is one of the most vital parts in a vehicle dynamic system. Designing, modeling and fabrication of tires depend on many factors as they have to support the weight of the vehicle, cushion the vehicle over surface irregularities, provide sufficient traction for driving and braking, and provide steering control and direction stability. Rubber is an essential material of the pneumatic tires as it offers flexibility, low hysteresis, high abrasion resistance, good impermeability to contained air and good friction on most surfaces. Tires are usually made of rubber with reinforcements embedded inside rubber. Since rubber is a viscoelastic material, it absorbs vibrations due to surface irregularities to a small extent. In other words, tire acts as damper. A vehicle tire transmits the vehicle load to the surface on which it rolls and at the same time provides the traction force for acceleration, braking etc and provides cornering force which gives stability to the vehicle while taking turns. These forces and moments have a great influence on the stability and efficiency of the vehicle. The tire forces and moments depend on many factors such as tire temperature, inflation pressure, contact pressure, the surface on which it rolls, vehicle path etc.

This thesis deals with the study of the effect of tire temperature on these forces and moments. Experimental determination of the forces and moments at different temperature is complex and expensive and it is difficult to maintain the tire temperature constant for the analysis. Hence we follow a hybrid approach to study the effect of temperature. For this, first, we make a finite element model in ABAQUS using the experimental results on a sample piece of rubber. Then we will do the steady state analysis at different temperatures using ABAQUS and will compare the results with modified PAC2002 model to extract the parameters. Subsequently we will use these parameters to do the transient analysis in ADAMS. Before going into

the detail of the thesis, the following sections give a brief idea of the tire structure, different tire models and different types of tire forces and moments acting on the tire-road interaction.

1.1 Tire Structure

The schematic diagram of a tire cross section is shown in fig. 1.1. It's main structural component is the carcass, which consists of layers of stiff cords to hold the shape of the tire and the tension from the compressed air. Carcass is made up of a series of layers of flexible cords of high modulus of elasticity encased in a rubber compound with low elastic modulus (plies). The cords are made of natural, synthetic or metallic materials and are anchored around the beads built with steel cords of high tensile strength[1]. High tensile steel wires, called beads, keep the carcass to the rim and when a load is applied on the wheel, the rim primarily hangs on the sidewall cords and the beads. The entire structure is covered with a wear resistant rubber compound, often styrene-butadiene, to protect the carcass and to build up the friction to the road.

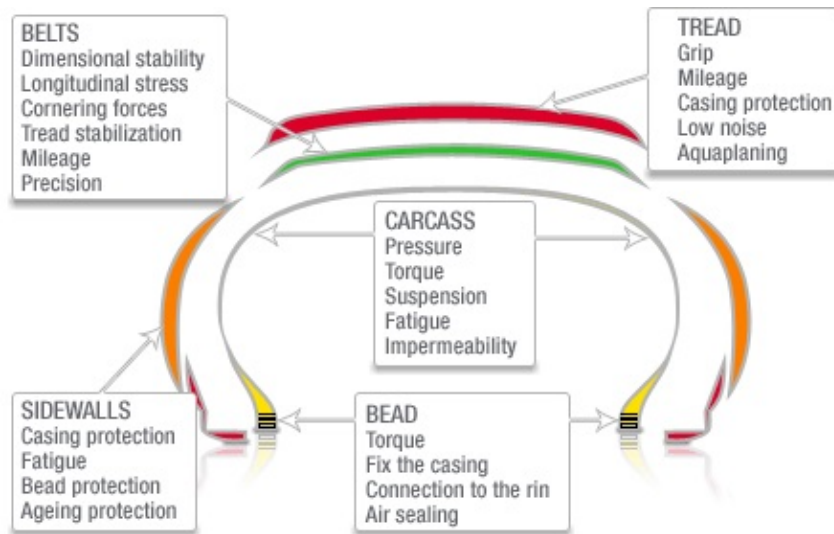


Figure 1.1: Tire Components and its Functions [1]

1.1.1 Types of Tire based on Tire Structure

The characteristics of the tire are largely dependent on the design and construction of the carcass. The direction of geometrical arrangement of the plies has a significant

role in the tire characteristics. Crown angle determines the direction of plies. Crown angle is the angle between direction of the steel cords that make up the plies and the center line of the circumference of the tire. Depending on the arrangement of the plies, the different existing types of tires can be divided into diagonal(cross) ply, radial ply and bias-belted.

Cross Ply Tires

In the cross ply tires, the carcass cords extend diagonally from bead to bead with a crown angle of about 40° . The number of plies is variable from a minimum of 2 (for low-load tires), to 20 (heavy duty). The cords in two adjacent plies run in opposite directions, overlapping and forming a diamond shape pattern (criss-cross). In operation, the diagonal plies flex and rub, elongating the diamond-shaped elements and the matrix rubber, this action produces a bending movement and friction between the tread and the road, which is a major cause of tire wear and rolling resistance. Therefore, radial tires are nowadays mostly used for cars and trucks, even though their manufacturing process is more complex and the expense is about 50 percent higher than that for a bias-ply tire [2].

Radial Tires

The radial tire differs from the cross ply tire by the crown angle. The radial tire has one or more layers of cords in the carcass that extend radially from bead to bead, thus having a crown angle of 90° . A belt is mounted beneath the tread . These belts are usually made up of layers of cords with a high modulus of elasticity. These cords are usually made of steel or other high strength materials. The belt cords are laid at a low crown angle up to 20° . The relative movement of the cords in radial tire is very small and hence a low power dissipation when compared to cross ply tire. Hence the life of the radial tire is almost twice as that of cross ply tire. The surface pressure over the entire contact area of radial tires is relatively uniform when compared to the cross-ply tire.

Bias-Belted Tires

There are also tires called bias-belted tires constructed by inserting belts in the tread of a tire with cross ply construction. The cords of the belt are made of materials with a higher modulus of elasticity than those in the cross ply. The belt tread offers

exceptional rigidity against distortion and reduces tread wear and rolling resistance compared to conventional tires. Generally belted tires have characteristics midway between those of the other tires considered. Now we discuss about the tire markings.

1.1.2 Tire Markings

Tire characteristics differ with the dimensions of tire, type of tire etc. So in order to distinguish the type of tires, there is a tire marking system which is accepted world wide. The information regarding the characteristics of tire construction and its dimensions must necessarily be placed by the manufacturer on the side of the tire. Knowing the meaning of the markings is essential to recognize the different types of tires and their characteristics. An example of 180/55 ZR17 73W tire is shown in fig. 1.2.

- 180 is the nominal width of the tire,
- 55 is the aspect ratio, i.e., the ratio between the nominal height of the shoulder and the nominal width of the tire,
- ZR indicates that the tire has a radial construction,
- 17 is the rim diameter in inches,
- 73 is the load index,
- W is the speed index.

1.2 Tire Forces and Moments

The different types of forces and moments acting on a rolling tire is shown in fig. 1.3(a). These forces are the shear forces developed on the tire road interaction surface and the moments are due to the offset of point of action of resultant from the center of point of contact. The different forces and moments acting on the rolling tire are longitudinal force, lateral force, normal force, normal reaction force, self aligning moment, overturning moment and rolling resistance moment. Of these forces and moments longitudinal force, lateral force and self aligning moment are predominant in the study of tire force analysis.

Motorcycle Tyre Markings Chart

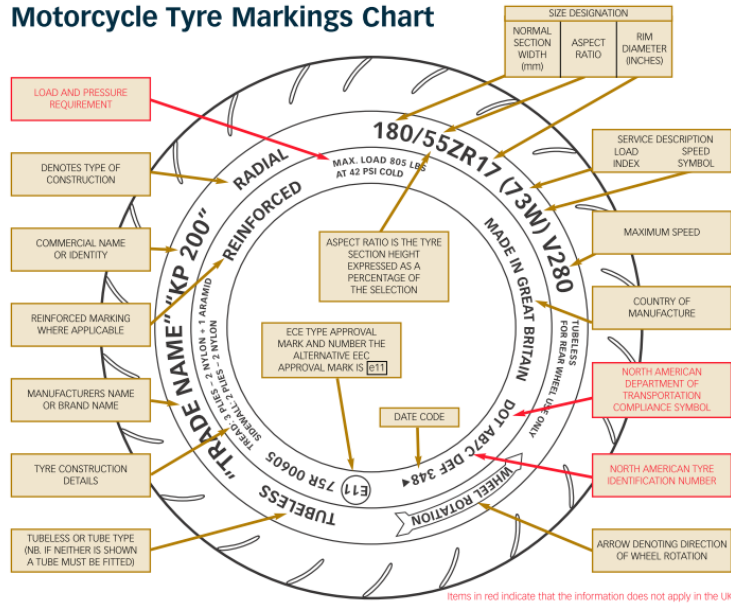


Figure 1.2: Tire Markings [1]

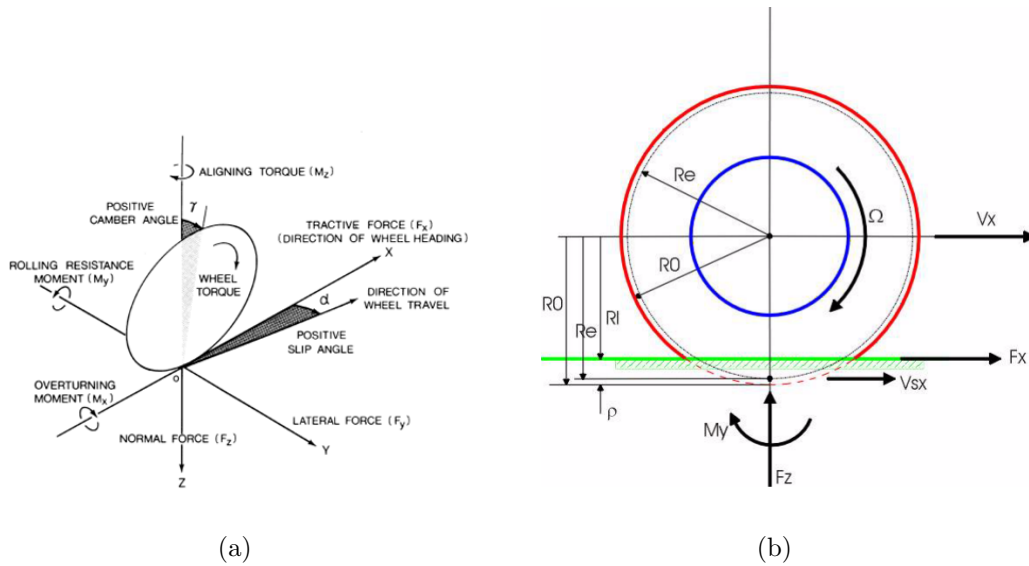


Figure 1.3: (a) Forces and Moments acting on a Rolling Tire [3], (b) Different types of Tire Radii [3]

1.2.1 Longitudinal Force

Longitudinal force is the shear force developed in the longitudinal direction or vehicle-moving direction. Longitudinal force is developed due to the difference in the wheel spindle velocity and the tangential velocity at the tire-road interaction. This difference in velocity is called longitudinal slip(V_{sx}). Longitudinal force is usually expressed in terms of slip ratio. Slip ratio(k) is defined as the ratio of slip speed to the velocity of the tire and is expressed as

$$k = -\frac{V_x - R_e\omega_w}{V_x} = -\frac{V_{sx}}{V_x} \quad (1.1)$$

where, R_e is the effective rolling radius, ω_w is the angular velocity of the wheel, and V_x , the longitudinal velocity of the tire axle. It is clear that the effective rolling radius has a significant influence on the slip ratio and hence the longitudinal force. The flattening of the tire takes place at the area of contact and the intensity of flattening depends on the torque supplied to the wheel. Hence it is difficult to find the effective rolling radius accurately. Jazar [4] in his works mentions that, the Tire Instant Effective Rolling Radius(TIER) is not equal to the unloaded radius nor to the radius when the vehicle is stationary with a static load. The effective rolling radius lies between the unloaded tire radius(R_0) and radius at static loaded condition(R_s). In his paper he proposed an expression to find the effective rolling radius. Figure 1.3(b) gives an idea of the the different types of radius.

$$R_e = \frac{2}{3}R_0 + \frac{1}{3}R_s \quad (1.2)$$

$$R_s = R_0 - \frac{F_z}{k_z} \quad (1.3)$$

$$R_e = R_0 - \frac{F_z}{3k_z} \quad (1.4)$$

where k_z is the vertical stiffness of the tire. This stiffness varies with the inflation pressure. The value of k_z can be found out experimentally or numerically. The slope F_z Vs ΔR gives the vertical tire stiffness. ΔR is the variation of instant effective radius around their nominal values R_{e0} .

$$\Delta R = R_e - R_{e0} \quad (1.5)$$

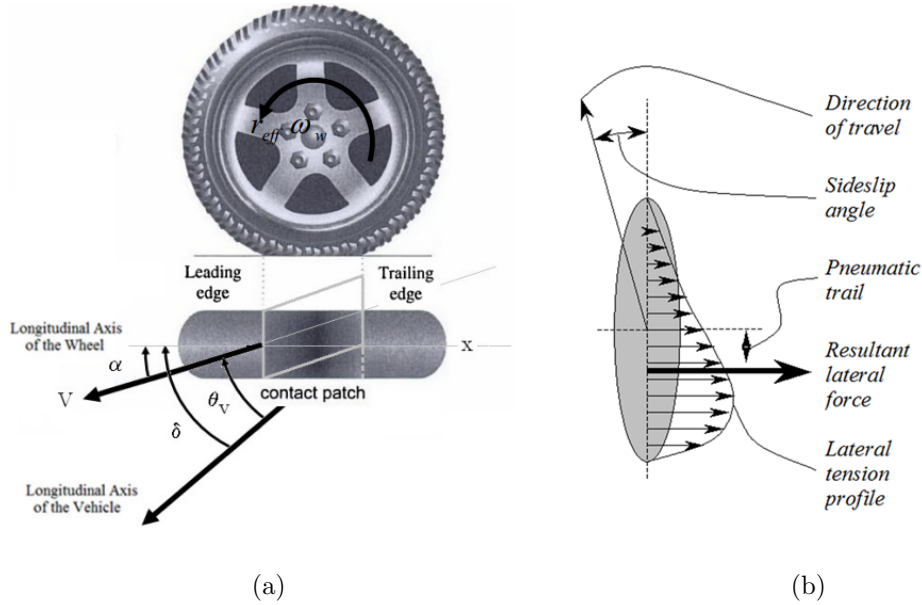


Figure 1.4: (a) Slip angle when the tire undergoes cornering [3], (b) Self alignment and pneumatic trail [3]

1.2.2 Lateral Force

Lateral force or cornering force is the contact shear force developed at the tire road interaction due to the change in the direction of motion of the vehicle and the direction in which wheel is pointing. The angle between these two directions is called slip angle(α). After giving a steering rotation of δ_o , the vehicle/tire is suppose to deflect at the same angle. But there will be slip in this angle as shown in fig 1.4(a). This slip angle(α) results in a slip in the lateral direction, which gives lateral force. The direction of this lateral force is perpendicular to the tire moving direction.

$$\alpha = \delta - \theta_v \quad (1.6)$$

where θ_v is the actual change in direction.

1.2.3 Self Aligning Moment

While taking a turn or cornering, the lateral shear stress distribution is not symmetric about the center of the patch and hence the resultant of the shear force(lateral force) acts at a point, some distance from the center of the patch. Self alignment moment is developed due to this offset of the point of action of resultant of lateral

force from the center of contact area. This offset is called pneumatic trail. Figure 1.4(b) gives an idea of the development of self alignment moment. This moment causes the tire to rotate, which opposes the slip angle and hence the name.

Other than the predominant forces and moments explained above, some other forces and moments also act on the tire due to the tire road interaction. They are rolling resistance moment and overturning moment. rolling resistance moment is the moment due to the uneven distribution of the vertical contact pressure over the contact area. Since the leading part of the tire at the contact area undergoes compression and the trailing part of the tire undergoes extension, the vertical resultant reaction force tends to shift toward the leading edge. Due to the offset and resultant reaction force from the ground, the moment can be developed against the tire rotational direction, and hence the name rolling resistance moment. Overturning moment is the moment due to the non-symmetric vertical pressure distribution acting on the tire spindle about the longitudinal axis across the tire width in the contact area. Now we discuss some tire models developed to extract these forces and moments.

1.3 Tire Models

In order to explain the tire characteristics many models have been developed. Some are theoretical models while others are empirical models based on tire measurement data. The empirical models are more accurate than pure theoretical models as the theoretical(physical) models could not incorporate all the slip, elastic and hysteresis phenomena of tire in motion. Brush model is an example of pure theoretical model. Empirical models are purely based on experimental results and there are a number of parameters which corresponds to all the phenomenon. The magic formula tire model ,PAC2002 model etc are examples of empirical models. A brief description of different tire models are as follows.

1.3.1 Brush Model

The brush model [5] , relies on the assumption that the slip is caused by deformation of the rubber material between the tire carcass and the ground. The material is approximated as small brush elements attached to the carcass, which is assumed to be stiff. The carcass can still flex toward the hub, but it can neither stretch nor

shrink. Every brush element can deform independently of the other.

1.3.2 Ftire Model

FTire (Flexible Ring Tire Model)[6] is a full 3-D nonlinear in-plane and out-of-plane tire simulation model. It is used by engineers in the vehicle and tire industry worldwide. FTire explains most of the complex tire phenomena on a mechanical, thermodynamical, and tribological basis. It is based on a structural dynamics based tire modeling approach. Ftire model describes the tire belt as an extensible and flexible ring carrying bending stiffness, elastically founded on the rim by distributed stiffness in radial, tangential, and lateral direction, respectively. To every belt element, a number of mass-less tread blocks are associated. These blocks carry nonlinear stiffness and damping properties in radial, tangential, and lateral direction. The radial deflections of the blocks depend on road profile, locus, and orientation of the associated belt elements. Tangential and lateral deflections are determined by the sliding velocity on the ground and the local values of the sliding coefficient. All the six components of tire forces and moments acting on the rim are calculated by integrating the forces in the elastic foundation of the belt. In this thesis, we use the modified PAC2002 models. Our objective is to study the variation of forces and moments with temperature.

1.4 Literature Review

Initial development of analytical models were mainly based on different simplifications of the tire behavior such as the string based tire models, ring based tire models, and beam-on-elastic foundation based tire models [7, 8]. Most of these tire models consider the tread as a pre-stressed string or a ring and the sidewalls as elastic foundations supporting the tread structure. Loo [7] developed an analytical tire model based on the flexible ring under tension with radially arranged linear springs and dampers to represent the tread band of the tire. The developed model was used to characterize the vertical load displacement of tire and its free rolling resistance. Allen et al [9] mentioned the importance of coupling the tire model with vehicle operating condition. Rotta [10] employed a circular membrane model to represent the sidewall softening effect to analyze the deformation of a tire on a flat surface. To further improve the flexible ring type tire model, Rhyne and Cron [11] proposed the inclusion of bending and shear deformations. Although, these analytical models

(also called as phenomenological models) have proved to be valuable to study the general dynamic behavior of tires, they are difficult to be used as a design tool for the tire encompassing various effects. Consequently, many tire companies specify the tire parameters with respect to an empirical tire model, which is called as the magic formula. Pacejka[3] and his colleagues have established such magic formulas based on measurement data to predict the longitudinal force, cornering force and aligning moment.

To capture tire deformation and its coupling effect with road surface, finite element modeling, FEM, of tire were introduced in early 1970 [12]. As FEM formulation and computer speed improved, more accurate FEM models were obtained. Ridha [13] developed a homogeneous tire-road model using three dimensional finite elements. Later, the effective use of three dimensional elements was described by Chang et al [14]. To include the surface effect accurately. Faria et al[15] included contact region in the modeling. Pottinger compared stress distribution of solid and pneumatic tires in the contact region. Danielson et al.[16] analyzed three dimensional tire model in cylindrical coordinate system to obtain the forces. Luchini and Popio [17] employed the transient dynamic rolling analysis to obtain the time-histories of strains including the rolling effect.

Many studies have been done on the effect of temperature on tire characteristics and many models were developed for the same. J.R. Cho et al [18] in his paper predicted numerically the rolling resistance and the temperature distribution of 3-D periodic patterned tire. According to them this rolling resistance is induced due to the hysteresis loss of viscoelastic rubber compounds. The hysteresis loss during one revolution was computed with the maximum principal value of the half-amplitudes of six strain components, and the temperature distribution of tire was obtained by the steady-state heat transfer analysis. The coupling between the hysteresis loss and the temperature owing to the temperature non linearity of the loss modulus of rubber compound was solved by a staggered iterative computation. In his work it has been found that the tire tread pattern gives rise to the significant effect on the rolling resistance and peak temperature and their distributions.

Tian Tang et.al [19] developed a finite element approach to computationally evaluate the temperature field of a steady-state rolling tire and track. He calculated the average temperature of tread and sidewall using a three dimensional thermal analysis software Radtherm and the results from Radtherm were in strong agreement with the results from ABAQUS. He also studied the effects of loading and velocity on

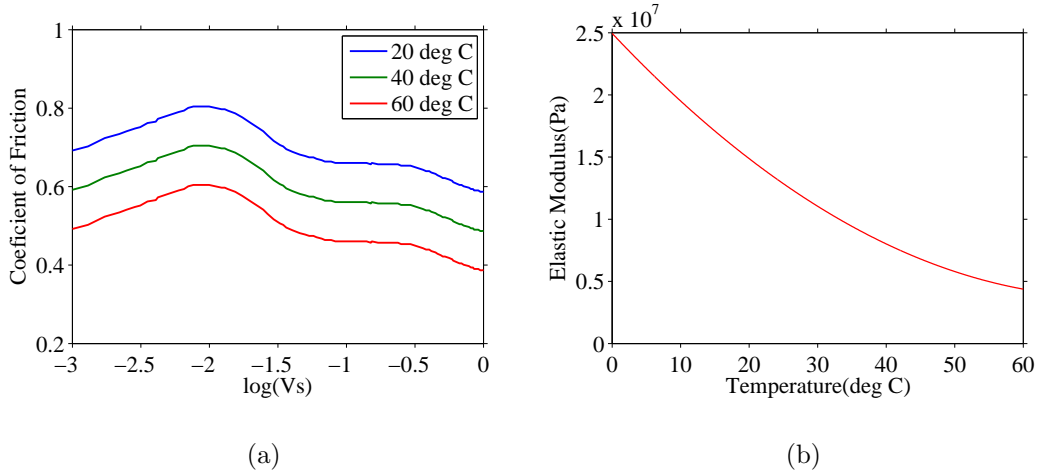


Figure 1.5: (a)Variation of coefficient of friction with sliding velocity at different temperature [22], (b)Variation of Elastic Modulus with temperature [20]

the temperature fields . But these thermal studies could not extract the steady state and transient response of these forces and moments, with the effect of temperature. Hence we follow a hybrid approach to extract these forces and moments. For this approach, we need the variation of material properties and coefficient of friction of tire rubber , considering temperature effects and slip.

D.D Higgins et al [20] investigated the friction process of styrene butadiene rubber(tire rubber). He has done experiments on a model tire rubber compound which contain 46 % styrene/butadiene. He has plotted the variation of elastic modulus with temperature from the experiments done on Tritec 2000 DMA apparatus as shown in fig. 1.5(b). The data were obtained by dynamic mechanical analysis in dual cantilever mode. Dynamic mechanical analysis or DMA [21] is a technique used to find the variation of visco-elastic properties with temperature,time,frequency etc. In this thesis we take into account this variation of elastic modulus with temperature for the material modeling in ABAQUS.

B N J Persson [22] studied the variation of rubber friction with temperature. This local heating is due to the visco-elastic energy dissipation. Based on his experiments, he explained the variation of friction with temperature for a particular slip velocity and also explained the variation of coefficient of friction with sliding velocity for a particular temperature. He has conducted experiments on tire tread rubber block sliding on a hard substrate. He has explained the profile of coefficient of friction with respect to sliding velocity for a temperature of $T=18^{\circ}C$. Assuming that the profile remains same at all temperatures we have extrapolated the varia-

tion of coefficient of friction with temperature and sliding velocity as shown in fig. 1.5(a). Korunovic et. al. [23] studied the variation of rubber friction with slip speed and contact pressure. He developed a Finite Element Model of tire and has done the tire force analysis and compared the numerical results with the experimental results. Later, Bibin et.al. [24] used this variation of rubber friction with slip speed and contact pressure to do the comparison of steady state and transient response of forces and moments of FEM model with experimental results. In this thesis we will consider the effect of temperature to do the steady state and transient analysis by using modified PAC2002 model.

1.5 Outline of the Thesis

After presenting the details of different tire models in chapter 1, we discuss the technique to include temperature effects in PAC2002 model in chapter 2. In chapter 3, we present methods to model the effective temperature related changes in the tire forces and moments using ABAQUS. Subsequently, we compute the parameters related with PAC2002 by comparing it with the numerical results at different temperature in chapter 3. Later, we do transient analysis of four wheel under the operating conditions of cornering, acceleration and braking in chapter 4. Finally, we conclude and present future direction for the present work.

Chapter 2

The Magic Formula PAC2002 Tire Model with Temperature effects

In this chapter we explain a semi empirical relation called Magic Formula PAC2002 and the modified version of this formula to capture the steady state forces and moments with the influence of temperature. It is difficult to mathematically model a tire to give the forces and moments acting on a tire road interaction accurately since these forces and moments depends on many parameters and variables. Many mathematical tire models are available such as brush model, HSRI model, lugre model which gives the tire forces and moments. In 1994 Hans B Pacejka [3] formulated a set of empirical relation based on experimental data(tire measurement data) which gives the steady state forces and moments more accurately than the other mathematical models. These set of equations, called "magic formula of tire" has been used commercially because of its accuracy. The magic formula to find the steady state forces and moments are expressed as

$$Y(X) = y(x) + S_v \quad (2.1)$$

$$y(x) = D \sin [C \arctan \{Bx - E (Bx - \arctan Bx)\}] \quad (2.2)$$

$$x = X + S_h \quad (2.3)$$

where, D , C , B , E are the magic formula's main parameters. These parameters are tuned to fit the magic formula curve with the tire measurement data. The value of these parameters gives an idea about the tire-road interaction surface, properties of tire etc. For example, the parameter D is the peak factor, which gives an idea of the coefficient of friction at the interaction. C is the shape factor, B is the stiffness

factor, E is the curvature factor. The product of parameters BCD, which is the slope of magic formula curve, gives the stiffness of the tire. S_v is the vertical shift and S_h is the horizontal shift of the curve due to side slip. Our study is confined to the longitudinal force (F_x), lateral force (F_y) and self alignment moment (M_z) which are predominant. The table given below gives an idea of the dependent quantities ($Y(X)$) and the independent quantities(X) of the magic formula. To make the

Independent quantity (X)	longitudinal slip(k)	slip angle(α)	slip angle(α)
Dependent quantity(Y)	Longitudinal Force (F_x)	Lateral Force (F_y)	Pneumatic trail(t) ($M_z = -t \times F_y$)

Table 2.1: Independent and Dependent Variables of Magic Formula.

magic formula more accurate, Pacejka modified the basic magic formula to bring it in strong agreement with the experimental results and this modified formula is called as PAC2002 model. In PAC2002 model, each main parameter depends on many sub parameters. The value of these parameters and sub parameters are obtained from tire measurement data. Most of the commercial vehicle dynamics simulation software use this model to do the tire analysis. In this thesis we deal with the effect of temperature on the tire forces and moments. To include the temperature effects on PAC model Masahiko M [25] modified the PAC2002 model and his model gives the lateral tire force with the influence of tire surface temperature. We have implemented the same approach to find the longitudinal force and self alignment moment. The modified PAC2002 model of Masahiko which gives the steady state lateral force taking account of temperature effects is expressed as follows.

2.1 Lateral Force at Pure Slip

Lateral force (F_y) is developed due to the existence of a side slip angle while cornering or taking a turn. Side slip angle or slip angle (α) is defined as the angle between the direction of travel of the tire and the direction of wheel plane. Temperature effects on Lateral forces are studied based of some assumptions listed below:

1. The variation of lateral force is proportional to the tire surface temperature,
2. The coefficient of dependency of tire surface temperature on the maximum side force has a different proportional value from that of the cornering power.

$$F_y(\alpha, T) = D_y(T) \sin [C_y \arctan \{B_y(T) \alpha_y - E_y (B_y(T) \alpha_y - \arctan B_y(T) \alpha_y)\}] + S_{V_y} \quad (2.4)$$

where,

$$\alpha_y = \alpha + S_{H_y} \quad (2.5)$$

$$C_y = p_{C_y1} \cdot \lambda_{C_y} \quad (2.6)$$

$$D_y = \mu_y \cdot F_z \cdot \zeta_2 \quad (2.7)$$

$$D_y(T) = D_y \cdot \{1 + \frac{\partial \mu_y}{\partial T} (T - T_m)\} \quad (2.8)$$

$$\mu_y = (p_{D_y1} + p_{D_y2} \cdot df_z) \cdot (1 - p_{D_y3} \gamma_y^2) \lambda_{\mu_y} \quad (2.9)$$

$$E_y = (p_{E_y1} + p_{E_y2} df_z) (1 + p_{E_y5} \gamma_y^2 - (p_{E_y3} + p_{E_y4} \gamma_y) \cdot \text{sgn}(\alpha_y)) \cdot \lambda_{E_y} \quad (2.10)$$

$$B_y(T) = \frac{K_y(T)}{(C_y \cdot D_y(T))} \quad (2.11)$$

$$K_y = p_{K_y1} \cdot F_{z0} \cdot \sin[2 \arctan(\frac{F_z}{p_{K_y2} \cdot \lambda_{F_{z0}} \cdot F_{z0}})] \cdot (1 - p_{K_y3} \cdot |\gamma_y|) \cdot \zeta_3 \cdot \lambda_{K_y} \cdot \lambda_{F_{z0}} \quad (2.12)$$

$$K_y(T) = K_y \cdot \{1 + \frac{\partial C_p}{\partial T} (T - T_m)\} \quad (2.13)$$

$$S_{H_y} = (p_{H_y1} + p_{H_y2} \cdot df_z) \lambda_{H_y} + p_{H_y3} \cdot \gamma_y \cdot \zeta_0 + \zeta_4 - 1 \quad (2.14)$$

$$S_{V_y} = F_z \cdot \{(p_{V_y1} + p_{V_y2} \cdot df_z) \lambda_{V_y} + (p_{V_y3} + p_{V_y4} \cdot df_z) \cdot \gamma_y\} \cdot \zeta_4 \cdot \lambda_{\mu_y} \quad (2.15)$$

$$\gamma_y = \gamma \cdot \lambda_{\gamma_y} \quad (2.16)$$

T_m is the ambient average tire surface temperature. The steady state tire forces analysis without elevated temperature is done at this temperature. D_y , E_y , K_y etc are the parameters of steady state tire lateral force model at T_m . $D_y(T)$, $B_y(T)$ and $K_y(T)$ are the parameter values including the effect of tire surface temperature.

$$\frac{\partial \mu_y}{\partial T} = \frac{d(D_y(T))/dT}{D_y} \quad (2.17)$$

$$\frac{\partial C_p}{\partial T} = \frac{d(K_y(T))/dT}{K_y} \quad (2.18)$$

where $d(D_y(T))/dT$ is equal to the gradient of peak value of lateral force with respect to time. The value can be calculated from the numerical results using ABAQUS. Table given below shows the variation of peak value of lateral force at different temperature. The variation of peak lateral force with temperature is shown in fig. 2.1(a). We will take the average value of the gradient of both positive(clockwise) and negative(counter-clockwise) slip angle condition. $\partial \mu_y / \partial T$ can also be taken from

Temperature (deg C)	Peak value of Lateral force(N) (for -ve slip angles)	Peak value of Lateral force(N) (for +ve slip angles)
20	-2615.65	2393.38
40	-2203.61	1977.23
60	-1799.22	1565

Table 2.2: Variation of peak Lateral Force with Temperature from ABAQUS

Temperature (deg C)	Lateral force(N) at $\alpha = -1^\circ$	Lateral force(N) at $\alpha = +1^\circ$
20	-1247.28	1026.01
40	-1114.58	890.867
60	-945.005	706.167

Table 2.3: Lateral Force (at $\alpha = 1^\circ$) at different Temperatures from ABAQUS

the variations of friction with temperature as shown in 1.5(a)

Similarly $d(K_y(T))/dT$ in equation. 2.18 is taken as the change of lateral force at slip angle of 1_o . The forces at different temperature are extracted from ABAQUS for a slip angle of 1° clockwise and anticlockwise direction and the gradient of force with respect to temperature is found out for both(+ve and -ve) 1° separately as shown in fig. 2.1(b) and averaged.

2.2 Longitudinal Force at Pure Slip

Longitudinal force (F_x) at the tire-road interface is due to the speed difference between tangential velocity of tire at the contact patch($R_e\omega_w$) and the velocity of the tire axle($R_0\omega_w$). Such differences in speed is called slip speed or slip velocity. The slip ratio (k) is defined as the ratio of slip velocity to free rolling velocity which is given by

$$k = -\frac{V_x - R_e\omega_w}{V_x}, \quad V_x = R_0\omega_w \quad (2.19)$$

where, R_e is the effective rolling radius, ω_w is the angular velocity of the wheel, V_x longitudinal velocity of the tire axle. Masahiko M modified the PAC2002 model for lateral forces only. Here in this paper we modify the PAC 2002 model to study the effect of temperature on longitudinal forces also. The modified PAC2002 model for longitudinal force is as follows.

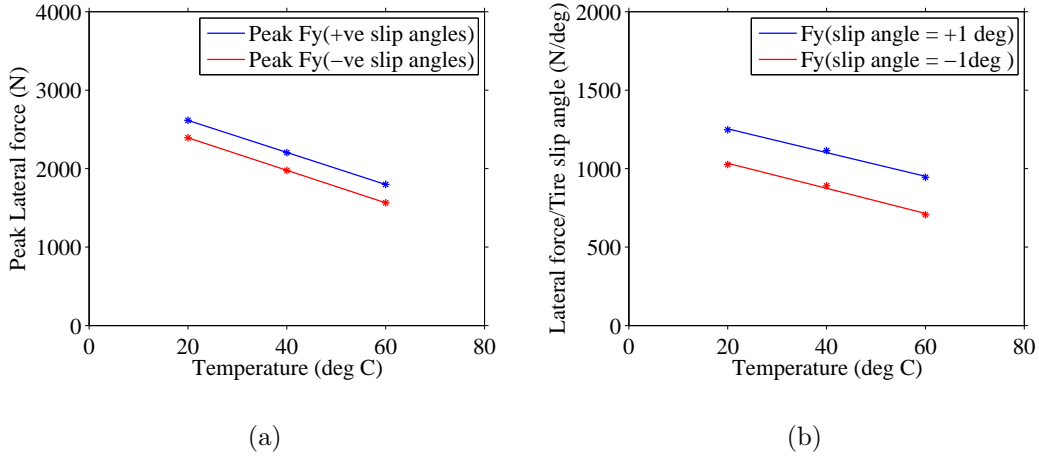


Figure 2.1: (a)Variation of peak Lateral Force with Temperature from ABAQUS, (b)Variation of Lateral Force with Temperature (at $\alpha = 1^\circ$) from ABAQUS

$$F_x(k, T) = D_x(T) \sin [C_x \arctan \{B_x(T)k_x - E_x (B_x(T)k_x - \arctan B_x(T)k_x)\}] + S_{Vx} \quad (2.20)$$

where,

$$k_x = k + S_{Hx} \quad (2.21)$$

$$C_x = p_{Cx1} \cdot \lambda_{Cx}$$

$$D_x = \mu_x \cdot F_z \cdot \zeta_1 \quad (2.22)$$

$$D_x(T) = D_x \cdot \left\{1 + \frac{\partial \mu_x}{\partial T} (T - T_m)\right\} \quad (2.23)$$

$$\mu_x = (p_{Dx1} + p_{Dx2} \cdot df_z) \cdot \lambda_{\mu x} \quad (2.24)$$

$$E_x = (p_{Ex1} + p_{Ex2} df_z + p_{Ex3} \cdot df_z^2) \cdot (1 - p_{Ex4} \cdot \text{sgn}(k_x)) \cdot \lambda_{Ex} \quad (2.25)$$

$$B_x(T) = \frac{K_x(T)}{(C_x \cdot D_x(T))} \quad (2.26)$$

$$K_x = F_z \cdot (p_{Kx1} + p_{Kx2} \cdot df_z) \cdot (\exp(p_{Kx3} \cdot df_z)) \cdot \lambda_{Kx} \quad (2.27)$$

$$K_x(T) = K_x \cdot \left\{1 + \frac{\partial C_p}{\partial T} (T - T_m)\right\} \quad (2.28)$$

$$S_{Hx} = (p_{Hx1} + p_{Hx2} \cdot df_z) \lambda_{Hx} \quad (2.29)$$

$$S_{Vx} = F_z \cdot (p_{Hx1} + p_{Hx2} \cdot df_z) \lambda_{Vx} \cdot \lambda_{\mu x} \cdot \zeta_1 \quad (2.30)$$

$$\gamma_x = \gamma \cdot \lambda_{\gamma x} \quad (2.31)$$

T_m is the ambient average tire surface temperature. The steady state tire forces analysis without elevated temperature is done at this temperature. D_x , E_x , K_x etc are the parameters of steady state tire lateral force model at T_m . $D_x(T)$, $B_x(T)$ and $K_x(T)$ are the parameter values including the effect of tire surface temperature.

$$\frac{\partial \mu_x}{\partial T} = \frac{d(D_x(T))/dT}{D_x} \quad (2.32)$$

$$\frac{\partial C_p}{\partial T} = \frac{d(K_x(T))/dT}{K_x} \quad (2.33)$$

where $d(D_x(T))/dT$ is equal to the gradient of peak value of longitudinal force with respect to temperature. The value can be calculated from the numerical results using ABAQUS. Table given below shows the variation of peak value of longitudinal force at different temperature. The variation of peak longitudinal force with temperature is shown in fig. 2.2(a). We will take the average value of the gradient on both positive(clockwise) and negative(counter-clockwise) slip angle condition. $\partial \mu_x / \partial T$ can also be taken from the variations of friction with temperature as shown in 1.5(a)

Temperature (deg C)	Peak value of Longitudinal force(N) (for -ve slip)	Peak value of Longitudinal force(N) (for +ve slip)
20	-2624.48	2609.21
40	-2214.65	2207.13
60	-1807.15	1798.49

Table 2.4: Variation of Peak Longitudinal Force with Temperature from ABAQUS

Similarly $d(K_x(T))/dT$ in equation. 2.33 is taken as the gradient of longitudinal force at 1 slip with respect to temperature. It is clear from the profile of steady state longitudinal curves that the variation of longitudinal forces at $k = .3$ is same as that at $k = 1$. In order to find the value of $d(K_x(T))/dT$ the longitudinal forces at different temperature are extracted from ABAQUS for a slip of +1 and -1 and the

Temperature (deg C)	Longitudinal force(N) at $k = -1$	Longitudinal force(N) at $k = +1$
20	-2375.011	2385.912
40	-1974.855	1990.495
60	-1574.715	1589.279

Table 2.5: Longitudinal Force (at $k= 1$) at different Temperatures from ABAQUS

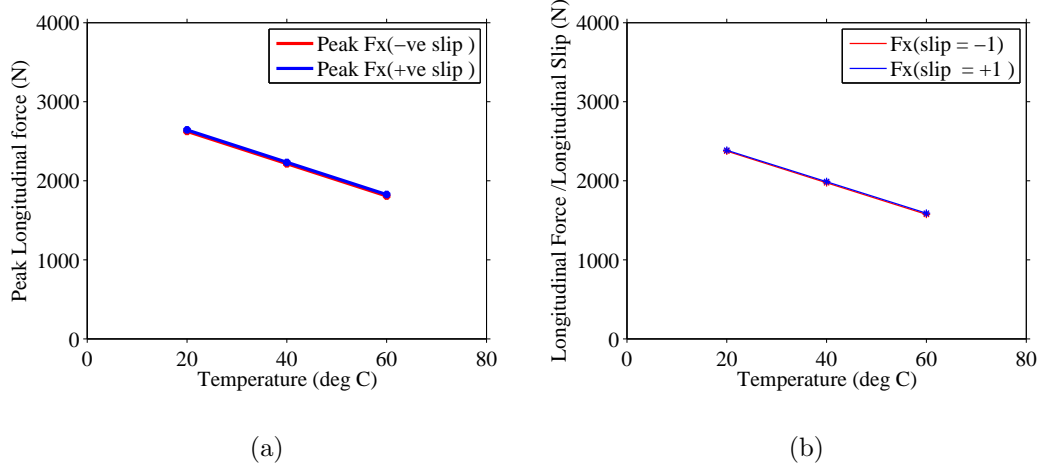


Figure 2.2: (a)Variation of Peak Longitudinal Force with Temperature from ABAQUS, (b)Variation of Longitudinal Force with Temperature (at $k = 1$) from ABAQUS

gradient is calculated for both cases separately as shown in fig. 2.1(b). The mean of the slopes of two lines gives the the value of $d(K_x(T))/dT$.

2.3 Self Aligning Moment at Pure Slip

The lateral force acting at the tire-surface interface is not symmetric about the wheel plane. It also induces a moment or torque, known as self alignment moment (M_z), about the vertical axis. Such moment tends to rotate the tire so as to minimize the effect of slip angle. The magnitude of the self alignment moment depends on pneumatic trail $t(\alpha)$ and residual moment, M_{zr} . The pneumatic trail also varies with temperature . Hence we modify the expression for pneumatic trail and the resulting pneumatic trail is termed as $t(\alpha, T)$ and the corresponding moment with the effect of temperature is termed as $M_z(T)$ The expression for the self aligning moment without the influence of temperature is

$$M_z = -t(\alpha) \cdot F_y + M_{zr} \quad (2.34)$$

and the expression for self alignment moment considering the temperature effects is expressed as

$$M_z(T) = -t(\alpha, T) \cdot F_y(T) + M_{zr} \quad (2.35)$$

$$t(\alpha) = D_t \sin [C_t \arctan \{B_t \alpha_t - E_t (B_t \alpha_t - \arctan B_t \alpha_t)\}] \quad (2.36)$$

$$t(\alpha, T) = D_t(T) \sin [C_t \arctan \{B_t \alpha_t - E_t (B_t \alpha_t - \arctan B_t \alpha_t)\}] \quad (2.37)$$

where,

$$\alpha_t = \alpha + S_{H_t} \quad (2.38)$$

$$C_t = q_{Cz1} \quad (2.39)$$

$$D_t = (q_{Dz1} + q_{Dz2} \cdot df_z) (1 + q_{Dz3} \gamma_z + q_{Dz4} \gamma_z^2) \frac{R_0}{F_z} \cdot \lambda_t \cdot \zeta_5 \quad (2.40)$$

$$D_t(T) = D_t (1 + \frac{dt_{peak}}{dT} (T - T_m)) \quad (2.41)$$

$$E_t = (q_{Ez1} + q_{Ez2} df_z + q_{Ez3} \cdot df_z^2) \quad (2.42)$$

$$B_t = (q_{Bz1} + q_{Bz2} df_z + q_{Bz3} \cdot df_z^2) (1 + q_{Bz4} \gamma_z + q_{Bz4} |\gamma_z|) \frac{\lambda_{Ky}}{\lambda_{By}} \quad (2.43)$$

$$S_{H_t} = (q_{Hz1} + q_{Hz2} \cdot df_z) (q_{Hz3} + q_{Hz4} \cdot df_z) \cdot \gamma_z \quad (2.44)$$

$$\gamma_z = \gamma \cdot \lambda_{\gamma z} \quad (2.45)$$

The residual moment (M_{zr}) can be expressed as

$$M_{zr} = D_r \cdot \cos [C_r \cdot \arctan (B_r \cdot \alpha_r)] \cdot \cos (\alpha) \quad (2.46)$$

$$\alpha_r = \alpha + S_{H_f} \quad (2.47)$$

$$S_{H_f} = S_{H_y} + \frac{S_{V_y}}{K_y} \quad (2.48)$$

$$C_r = \zeta_7 \quad (2.49)$$

$$D_r = F_z \cdot [(q_{Dz6} + q_{Dz7} \cdot df_z) \cdot \lambda_r + (q_{Dz8} + q_{Dz9} \cdot df_z) \cdot \gamma_z] \cdot R_0 \cdot \lambda_{\mu\gamma} + \zeta_8 - 1 \quad (2.50)$$

$$B_r = (q_{Bz9} \cdot \frac{\lambda_{Ky}}{\lambda_{Ky}} + q_{Bz10} \cdot B_y \cdot C_y) \cdot \zeta_6 \quad (2.51)$$

$$df_z = \frac{F_z - F'_{z0}}{F'_{z0}}, \quad F'_{z0} = F_{z0} \times \lambda_{F_{z0}} \quad (2.52)$$

where dt_{peak}/dT is the variation of peak pneumatic trail with temperature. We will find its value from ABAQUS. From ABAQUS, first we extract the peak value of self aligning moment at three different temperatures. Then we can find the pneumatic trail by dividing the extracted peak self aligning moment with the lateral force at corresponding slip angle, considering temperature effect. This process is done for positive and negative slip angles and the mean of slope of pneumatic trail vs temperature at positive and negative slip angles gives the value of dt_{peak}/dT .

In the PAC2002 model, F_z and F_{z0} are normal load and nominal load respectively. p_{Cx1} , p_{Dy2} , p_{Ez3} etc., are sub parameters which control the variation of main parameters (C_x , D_y , E_t etc) with different conditions such as variation of load, inclination angle, residual moment etc. λ_{Cx} , λ_{By} etc are the scaling factors of main parameters and other inputs of magic formula such as camber angle, μ_y etc. x , y , and z in the suffix indicates that the parameters or sub parameters are associated with the forces along x and y directions, and moment about z direction, respectively. The p in the sub parameter denotes the forces at pure slip while that with q denotes the moment at pure slip. ζ_i is the reduction factor. Since, turn-slip is neglected for steady state pure slip condition and small camber, the value of ζ_i can be set to 1. R_0 is the unloaded wheel radius. γ is the roll angle or camber angle which is neglected in our analysis.

2.4 Summary

In this chapter we have explained the basic magic formula of tire, the PAC2002 model and the modified PAC2002 model. Mazahiko et. al, has modified the PAC2002 model to include temperature effects on lateral force which is shown in section 2.1. We have followed the same procedure to modify the longitudinal force and self aligning torque. The expression for pneumatic trail is modified to include the temperature effects in self aligning moment. In the next section, we present the Finite Element Modeling and Analysis of a tire with temperature effects.

Chapter 3

Steady State Analysis - FEM Approach

In this chapter we discuss the finite element modeling and analysis of the tire and compare the FEM results with modified PAC2002 model. First we will model a tire and the road on which tire rolls in ABAQUS and will apply loads and boundary conditions. Then this model is given motion and the forces and moments acting on the tire-road interaction are extracted. These forces and moments from ABAQUS are compared with the results from modified PAC2002 model considering temperature effects. Then these models will be used for transient analysis which will be explained in next chapter. The details of the finite element model are explained as follows.

3.1 FEM Modeling

The FEM modeling and analysis of tire is done using ABAQUS[26][27][24]. We model different components such as carcass, sidewall, belt, tread, membrane belt, etc. with appropriate materials and elements. Rubber is used to model tread and sidewalls where as fiber reinforced rubber composites is used to model carcass and belt. The rubber used in the tire is modelled as an incompressible hyper elastic material model which includes a time domain viscoelastic component and the fiber reinforced in the fiber reinforced rubber composites is modeled as a linear elastic material. The time-domain viscoelastic component is defined by a Prony series expansion of the relaxation dimensionless modulus with relaxation time of 0.1. This component is employed to incorporate the stress relaxation w.r.t time at constant

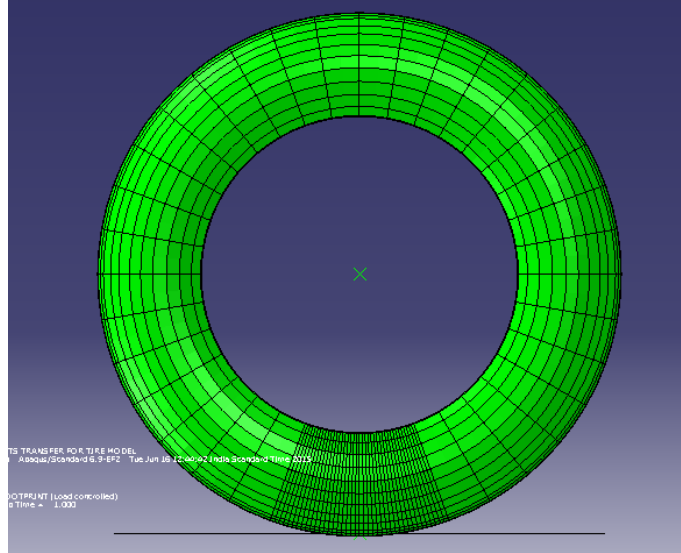


Figure 3.1: A 3-dimensional tire model in ABAQUS

strain. That is, for when a material is subjected to a sudden strain and kept constant over the duration of the test, the stress relaxes over time. Long term parameter is used with hyperelastic model to incorporate long term behaviour of the rubber. The variation of elastic modulus of rubber with temperature is also considered and the variation is taken from the experiments done by D.D Higgins et al [20] on a sample piece of tire rubber.

The half section of the three dimensional model is first generated from axisymmetric model. The axisymmetric tire model is discretized with CGAX4H and CGAX3H elements. The belts and ply are discretized with SFMGAX1, modeled with rebar in surface elements embedded in continuum elements (rubber). The three dimensional model is obtained by reflecting half of the partial three dimensional tire model about the plane normal to axis of revolution. The partial three-dimensional model is generated by revolving the axisymmetric model cross-section about the rotational symmetry axis. Road is modeled as a rigid surface.

The hard contact is used to model the contact between the tire and the road since this contact relationship minimizes the penetration of slave surface(tire) into the master surface(road) at the constraint locations. Instead of giving a vertical load (negative-z direction) on the tire axle, a load is applied on the road in upward (positive-z) direction. Finally, to consider the inflation pressure, we apply uniform pressure of 220 kPa in the inner surface of the tire. Under the influence of such pressure, the tire experiences circumferential deformation which creates three

dimensional stress field with non-varying stresses in the circumferential direction.

The steady state rolling analysis of the tire is done based on Coupled Eulerian-Lagrangian(CEL) formulation. In this formulation, the tire rotation and movement are considered in Eulerian frame, and the deformation is considered in Lagrangian frame. Consequently, the steady moving contact problem is transformed into a pure spatially dependent simulation. In this formulation, contact region(40°) is more important and is meshed with more number of linear solid elements (C3D8H and C3D6H). Since the contact region has dense nodes and each element may be assumed to undergo a small deformation, we use linear elements in order to reduce the computation time. Rest of the tire section (i.e., 320°) is modeled with cylindrical elements (CCL12H and CCL9H) with relatively sparse nodes to cover large sectors with small number of elements.

3.2 Steady State Rolling Analysis

We perform steady state analysis of the tire(based on CEL formulation) under a vertical load of 4 kN acting on the tire axis . In this analysis, the ground velocity of the tire is 10 km/h (2.7778 m/s). The coefficient of friction (μ_r) of the rubber tire at the tire-road interaction varies with the temperature and slip speed. As discussed earlier we take the variation of friction coefficient from the experiments done by D.D Higgins et al [20] on a tire rubber sample at various temperatures and slip speeds. We incorporate these coefficient of friction values for the FEM modeling and analysis in ABAQUS as shown in table 2.2. The variation of elastic modulus of tire rubber with temperature is also taken into account from the experiments done by Higgins et. al and is shown in table 2.2. The lateral and longitudinal forces are the frictional shear forces acting on the contact area and self alignment moment is the product of the resultant of the lateral force and the offset of the line of action of resultant from the center of point of contact at zero cornering condition.

3.2.1 Steady State Lateral Force

In order to extract the lateral force from ABAQUS, we have to consider the variation of coefficient of friction with lateral slips and temperature. As discussed earlier we make use of the coefficient of friction values and elastic modulus values from the experiments done by B N J Persson [22] on a sample piece of tire rubber at

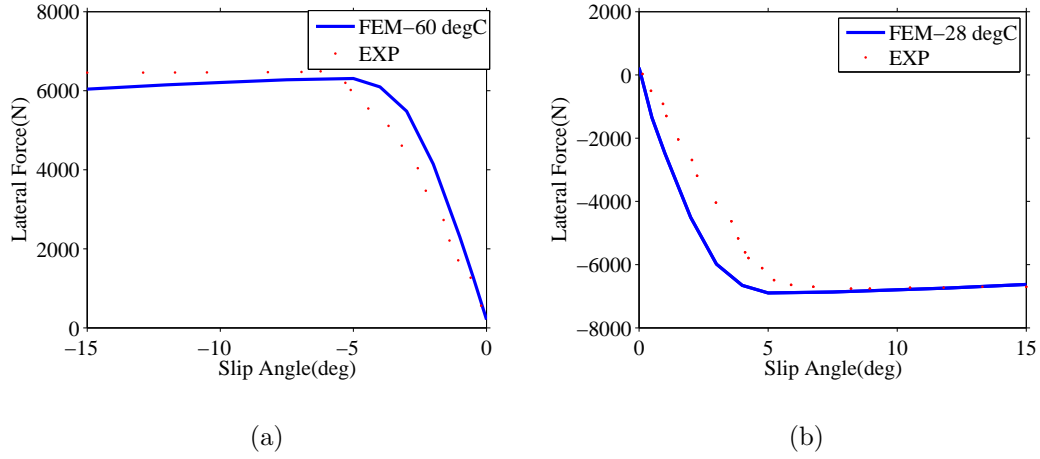


Figure 3.2: Validation of FEM results with experimental results [25]. (a) Validation for negative slip angles, (b) Validation for positive slip angles

different temperatures. Table 3.1 shows the variation of μ from the experiments corresponding to different slip speeds. In this case the slip speed is the lateral slip speed (V_{sy}) corresponding to each slip angle. The lateral slip speed of a tire taking a turn with a velocity, V , is expressed as:

$$\text{Lateral Slip Speed, } V_{sy} = V_y = V \sin(\alpha) \quad (3.1)$$

In this section, we will first validate FEM analysis results from ABAQUS with the Mazahiko et al's study of lateral force with the effect of temperature. To do the FEM analysis, we need the coefficient of friction, corresponding to the tire road interaction from their experiments. So we will extract the μ value from the experimental results. We take the μ corresponding to peak lateral force $\mu_{peak} = F_{y_{peak}}/F_z$ and assume the variation of μ is as same as shown in fig. 1.5(a). The validation is done for positive slip angles from -15° to 15° . The vertical load acting on the tire axis is 4600N. Figure 3.2(a) and fig.3.2(b) show the comparison of FEM model with the Mazahiko's experimental results. There is a slight variation of both the results from -5° to 5° . The slope of the curves in this region indicates the stiffness of the tire. While doing experiments with elevated temperatures, the lateral stiffness of the tire decreases correspondingly. The variation in slopes exists due to this decrease in lateral stiffness. And we can see from the graph that the peak values of forces are different for negative and positive slip angles. This is because Mazahiko has done the analysis at higher temperatures on negative slip angles than positive slip

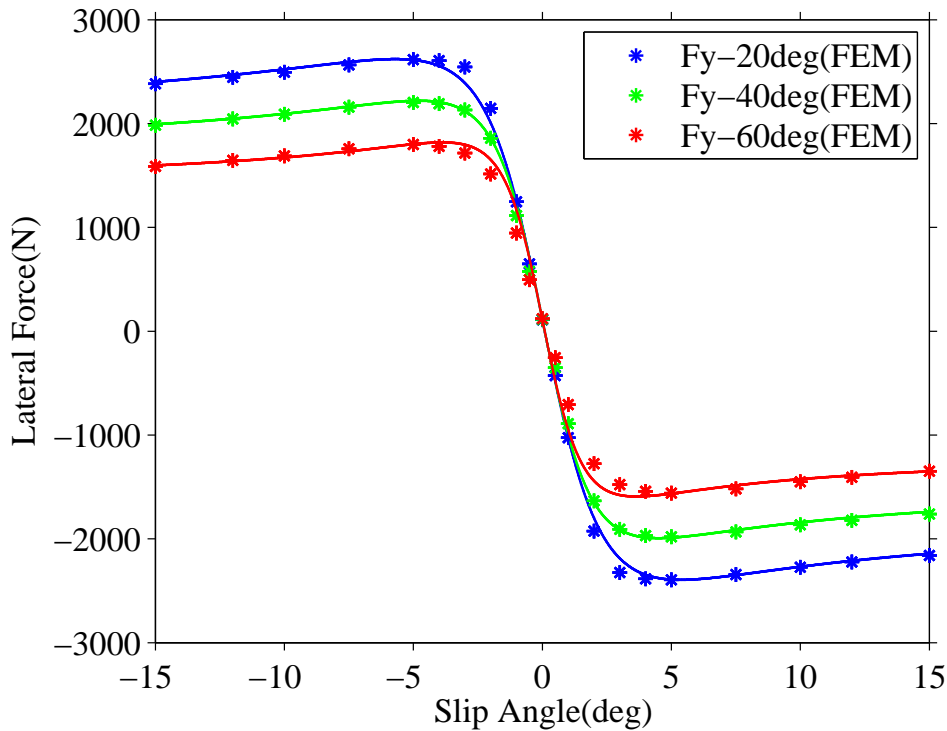


Figure 3.3: Variation of lateral force versus slip angle at different temperatures-FEM and modified PAC2002 model

angle. So we have also done FEM analysis at two different temperatures for +ve and -ve slipangles for validation. From fig. 1.5(a), it is evident that the coefficient of friction of tire rubber decreases with increase in temperature and hence two different peaks for +ve and -ve slip angles. Also we can see a difference in the lateral force around -15° . The reason is that we have considered the linear variation of friction with temperature for a slip speed of 1 m/s. From experiments it is evident that the at higher temperatures(above 40°) the variation of friction becomes nonlinear with temperature.

After validation we do the steady analysis in ABAQUS on a tire with a vertical load of 4000N acting on it. The steady state lateral force from ABAQUS is shown in fig. 3.3. In this figure, the FEM results from ABAQUS at various temperatures is compared with the modified PAC2002.

3.2.2 Steady State Longitudinal Force

To do the steady state longitudinal force analysis we have to give the longitudinal slip to the tire. The velocity of the tire axle is 10km/hr. For that linear velocity we

Slip Angle (α) in degrees	Component of V in Longitudinal direction (V_x) in m/s	Component of V in Lateral direction (V_y) in m/s	Coefficient of fric at 40°C(μ_{40})	Coefficient of fric at 40°C(μ_{40})	Coefficient of fric at 40°C(μ_{40})
0	2.7778	0	0.692024561	0.592024561	0.492024561
0.5	2.7777	0.024240627	0.692024561	0.592024561	0.492024561
1	2.7774	0.048479408	0.741147368	0.641147368	0.541147368
2	2.7761	0.096944049	0.677989474	0.577989474	0.477989474
3	2.7740	0.145379159	0.660445614	0.560445614	0.460445614
4	2.7710	0.193769985	0.656936842	0.556936842	0.456936842
5	2.7672	0.242101787	0.656936842	0.556936842	0.456936842
7.5	2.7540	0.3625765	0.642901754	0.542901754	0.442901754
10	2.7356	0.482361024	0.625357895	0.525357895	0.425357895
12	2.7171	0.577538425	0.614831579	0.514831579	0.414831579
15	2.6831	0.718949186	0.600796491	0.500796491	0.400796491

Table 3.1: Coefficient of Friction [22] w.r.t to Temperature and Slip Speed

find the effective rolling radius. For free rolling (i.e. without any torque on the tire) we will find the angular velocity of the tire. Free rolling condition happens, when the longitudinal force acting on the tire road interaction tends to zero. This can be done by trial and error method. The radius corresponding to this free rolling condition is called effective rolling radius. Longitudinal slip can be given to the tire by giving an angular velocity different from that of the angular velocity corresponding to free rolling. The different angular velocity applied to acquire different longitudinal slips is given in table.3.2. Then we incorporate the variation of coefficient of friction with longitudinal slips and temperature to extract longitudinal force. Table 3.2 shows the variation of μ . The steady state longitudinal force from ABAQUS for different slips is shown in fig. 3.4 . These results are compared with our modified PAC2002 model (refer section 2.2).

3.2.3 Steady State Self Aligning Moment

As already explained, self alignment moment is the product of the resultant of lateral force and the pneumatic trail. Since $M_z = -t \times F_y$, it depends on pneumatic trail and the variation of this pneumatic trail with the effect of temperature is neglected. To find the resultant moment due to the lateral force about the center contact point, we will find the sum of the product of lateral force (shear force in the lateral direction) at each node with the perpendicular (longitudinal distance) of the center of contact

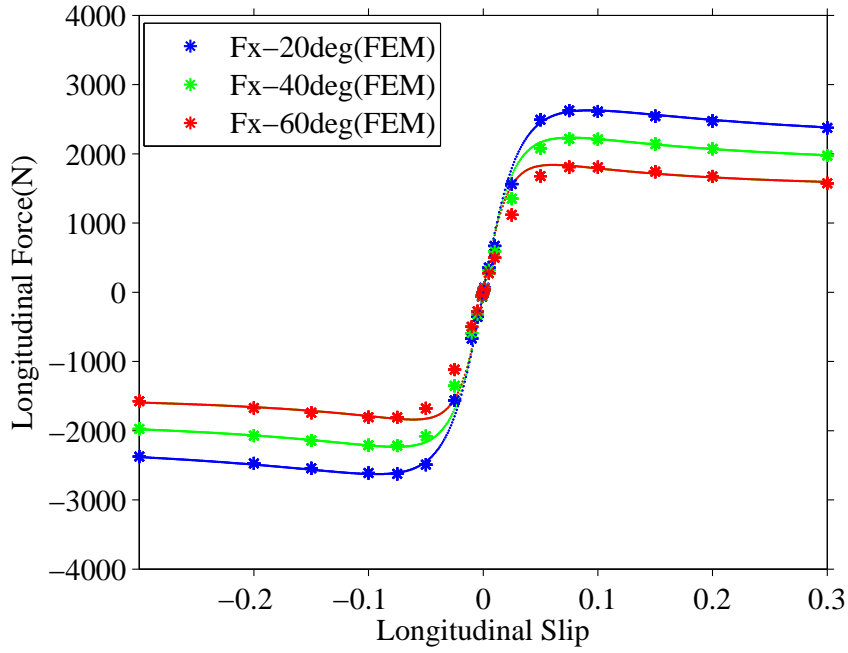


Figure 3.4: Variation of Longitudinal Force versus Slip Ratio at different Temperatures-FEM and modified PAC2002 model

point at zero slip to line of action of action of lateral force at corresponding slip angle on that node. The steady state self alignment moment from the FEM at three different temperatures(20°C, 40°C and 60°C) is compared with the modified PAC2002 model(refer section 2.3) as shown in fig. 3.5. In the figure it can be seen that the peak location and the variation of peak values with temperature, from ABAQUS are in strong agreement with modified PAC2002. The curvature of FEM model is different from that of the modified PAC2002 model because we are not considering the variation of lateral stiffness in FEM. As a result the slope of the curves are high in FEM model and the variation of slopes with temperature is also negligible.

3.3 Summary

In this chapter, we have done the steady state analysis in FEM with the effect of temperature. In order to incorporate the temperature effect we have considered the variation of coefficient of friction w.r.t temperature and slip speed. Also we have considered variation of elastic modulus of tire rubber with temperature. These variations were taken from the experiments done on a sample piece of tire rubber. Then

Slip (k)	Slip speed(V_s) in m/s	Coefficient of fric at 20°C(μ_{20})	Angular velocity at 20°C (ω_{20}) in rad/sec	Coefficient of fric at 40°C(μ_{40})	Angular velocity at 40°C (ω_{40}) in rad/sec	Coefficient of fric at 60°C(μ_{60})	Angular velocity at 60°C (ω_{60}) in rad/sec
0	0.00000	0.69202	9.01001	0.59202	9.02450	0.49202	9.03130
0.0005	0.00139	0.70255	9.00550	0.60255	9.01999	0.50255	9.02679
0.001	0.00278	0.74816	9.00100	0.64816	9.01548	0.54816	9.02227
0.002	0.00556	0.78325	8.99199	0.68325	9.00645	0.58325	9.01324
0.003	0.00833	0.80431	8.98298	0.70431	8.99743	0.60431	9.00421
0.005	0.01389	0.79378	8.96496	0.69378	8.97938	0.59378	8.98615
0.01	0.02778	0.73062	8.91991	0.63062	8.93426	0.53062	8.94099
0.015	0.04167	0.68852	8.87486	0.58852	8.88913	0.48852	8.89583
0.025	0.06945	0.66395	8.78476	0.56395	8.79889	0.46395	8.80552
0.05	0.13889	0.66045	8.55951	0.56045	8.57328	0.46045	8.57974
0.075	0.20834	0.65694	8.33426	0.55694	8.34766	0.45694	8.35395
0.1	0.27778	0.65343	8.10900	0.55343	8.12205	0.45343	8.12817
0.15	0.41667	0.63588	7.65850	0.53588	7.67083	0.43588	7.67661
0.2	0.55556	0.61834	7.20800	0.51834	7.21960	0.41834	7.22504
0.3	0.83334	0.59378	6.30700	0.49378	6.31715	0.39378	6.32191

Table 3.2: Coefficient of Friction [22] w.r.t to Temperature and Slip Speed and Angular Velocity given to tire at different Temperature and Slip Speed

we tuned the modified PAC2002 model parameters. It has been found out that the variation of forces and moments with temperature from ABAQUS is in agreement with that we got from modified PAC2002 model. The next step is to use these steady state models at different temperatures(20°C, 40°C, 60°C) to find the transient forces and moments under the influence of temperature.

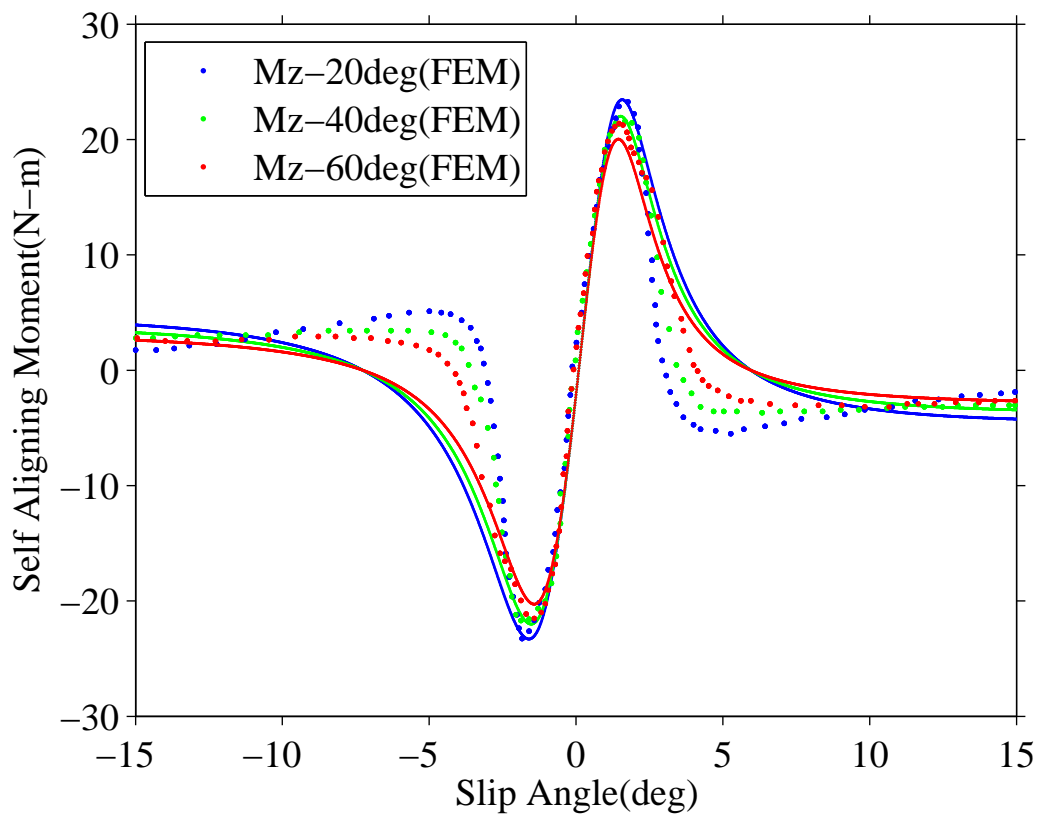


Figure 3.5: Variation of Self Aligning Torque versus Slip Angle at different Temperatures-FEM and modified PAC2002 model

Chapter 4

Transient Analysis with the effect of Temperature

This chapter deals with the study of the effect of temperature on the transient analysis of tire. Experimental determination of transient forces and moments at various temperatures is very complex and expensive and it is difficult to maintain a constant tire-surface temperature while doing the analysis. To overcome these difficulties we explain a hybrid approach to find these transient forces and moments using ADAMS Car Model. We will find the transient forces and moments at different temperatures for the three different maneuvers of Double Lane Change(DLC), acceleration and braking using each of the above said models.

4.1 ADAMS Transient Model:

This section deals with the transient analysis of the tire using a multibody dynamics software, MSC ADAMS[28]. ADAMS is the most widely used motion analysis software. ADAMS solve equations of Statics, Quasi-statics, Kinematics and Dynamics simultaneously and is also capable of running nonlinear dynamics in a tiny fraction of the time required by FEA solutions. Here, in this paper we make three different steady state tire models(corresponding to 20^oC, 40^oC and 60^oC). These steady state tire models are called tire property files. The parameters in this steady state tire models are tuned so that the steady state forces and moments from these models exactly match with the results in section 3.2. These parameter vales are taken from the PAC2002 model explained in the same section. For example with the effect of temperature the value of parameter has changed from D_y to $D_y(T)$.

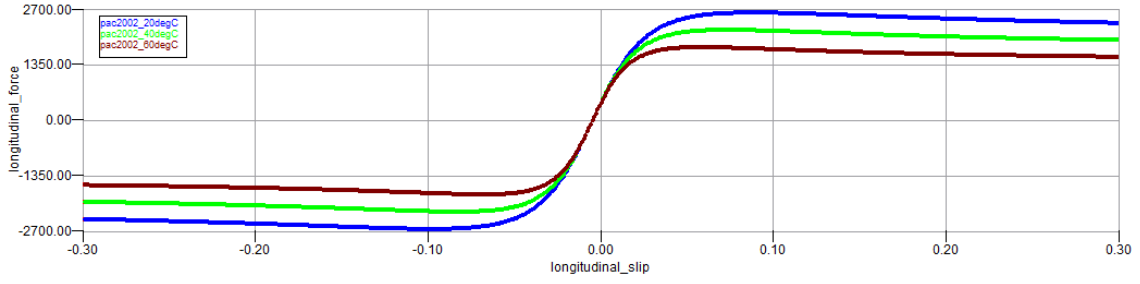


Figure 4.1: Steady State Longitudinal Forces at different temperatures

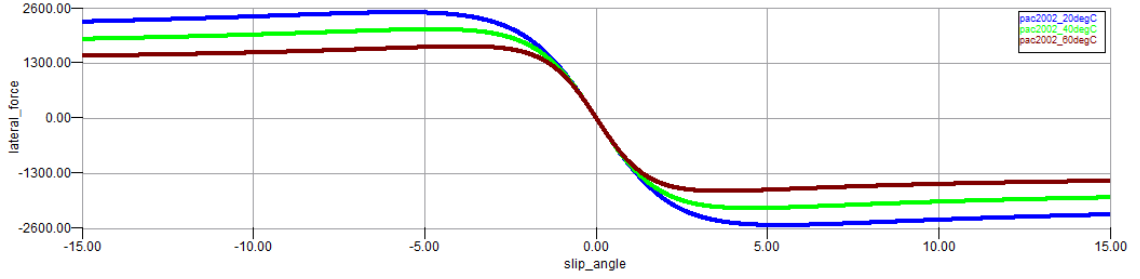


Figure 4.2: Steady State Lateral Forces at different Temperatures

It is clear from the Masahiko's model that the variation of parameter D is due to change in friction at lateral slip corresponding to peak lateral force. So the sub parameter to be changed is p_{Dy1} in ADAMS. The value of p_{Dy1} is tuned in ADAMS, so that the value of D_y which we calculate from ADAMS using equation 2.7 and equation 2.9, should be equal to the value $D_y(T)$ from modified PAC2002 in section 2.1. Similarly other parameters are also tuned in ADAMS. Then the steady state analysis results from ADAMS for a particular temperature is validated with modified PAC2002 results and FEM results in section 3.2. This method is employed for each of the three temperatures to form three different tire property files. The steady state response of these tire models using the three different tire models are shown in fig. 4.1, fig. 4.2 and fig. 4.3. Then these steady state tire models are incorporated in a demo car model in ADAMS to do the transient analysis at different temperatures. The specifications of the demo car used to do the transient analysis is given in Table. 4.1 and the wire frame model of the car is shown in fig. 4.4. We will do acceleration analysis, braking analysis and cornering analysis using this car.

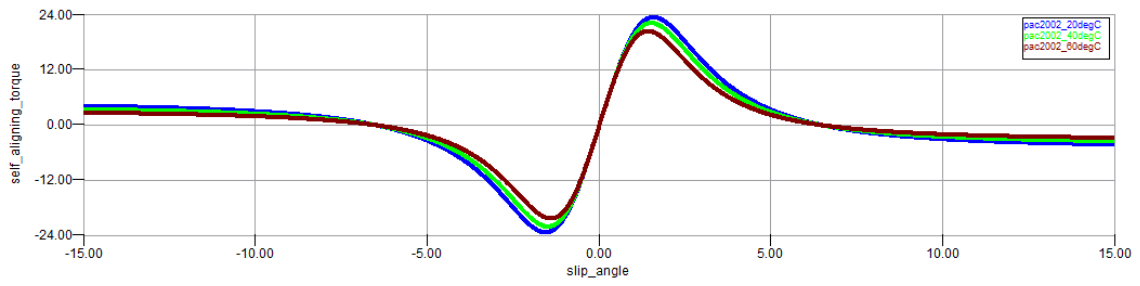


Figure 4.3: Steady State Self Aligning Moment at different Temperatures

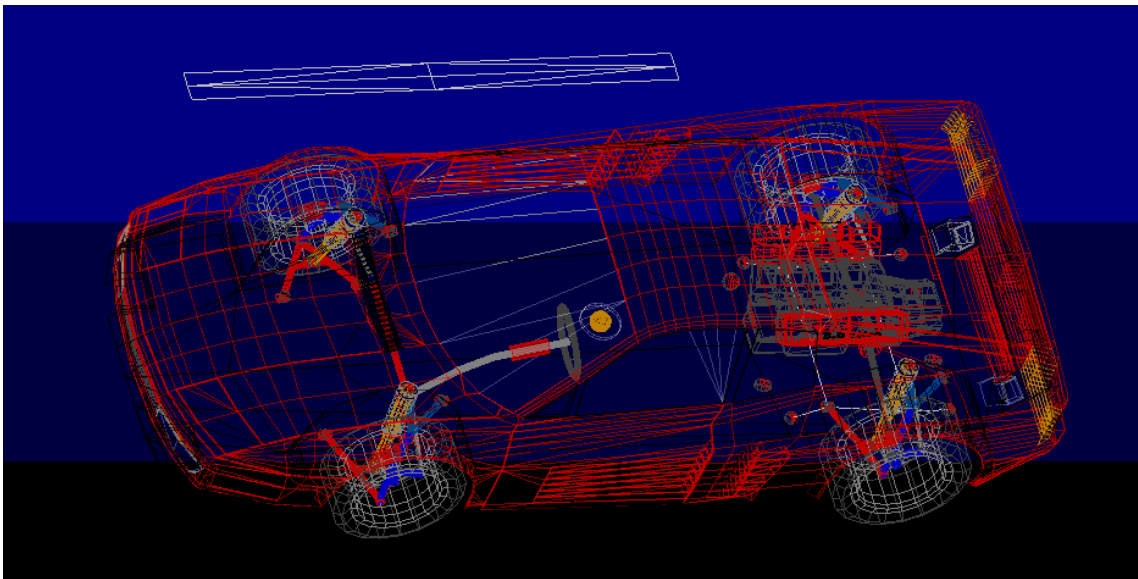


Figure 4.4: Wire frame model of the demo car in ADAMS

Sl. No	Specification	Values	Units
1	Mass of the car	995	kg
2	I_{xx} of the car	2×10^8	kg-mm ²
3	I_{yy} of the car	5×10^8	kg-mm ²
4	I_{zz} of the car	6×10^8	kg-mm ²
5	$I_{xy}=I_{yz}=I_{zx}$ of the car	0×10^8	kg-mm ²
7	Mass of the tire	50	kg
8	I_{xx} of the tire	3.133×10^5	kg-mm ²
9	I_{yy} of the tire	5.8×10^5	kg-mm ²
10	I_{zz} of the tire	3.134×10^5	kg-mm ²
11	$I_{xy}=I_{yz}=I_{zx}$ of the tire	0×10^5	kg-mm ²
12	Unloaded tire radius	316.57	mm
13	Rim radius	186.38	mm
14	Tire width	185.63	mm
15	Rim Width	129.11	mm
16	Aspect Ratio	0.703	-

Table 4.1: Car and Tire Specifications

4.1.1 Cornering Analysis

The objective of the cornering analysis in ADAMS is to find the transient response of lateral force and self aligning moment with respect to slip angles. There are many maneuvers which causes a change in the slip angle. In our analysis we consider Double Iso Lane Change(DLC) maneuver. To do the transient analysis using user defined tire models, the steady state tire property files created at three different temperatures are substituted for the default tire in the ADAMS car separately to form three different analysis. Thus we will do three different transient analysis at three different temperatures. The analysis is done on the car, moving with uniform velocity of 40km/hr and following a DLC maneuver. The step size given is 0.1 and the simulation is done in the third gear. Figure. 4.5 and fig. 4.5 explains the transient variation of lateral force and self aligning moment respectively. It can be seen that the peaks occur when the variation of slip angle changes as the direction of the steering wheel rotation changes. When the temperature increases, the peak value of lateral force and self aligning moment decreases. This is because of the decrease in the coefficient of friction with increase of temperature. When rotation of steering wheel changes direction, the lateral slip will be more and the hence the peak at this point and also the variation of the peak is more here.

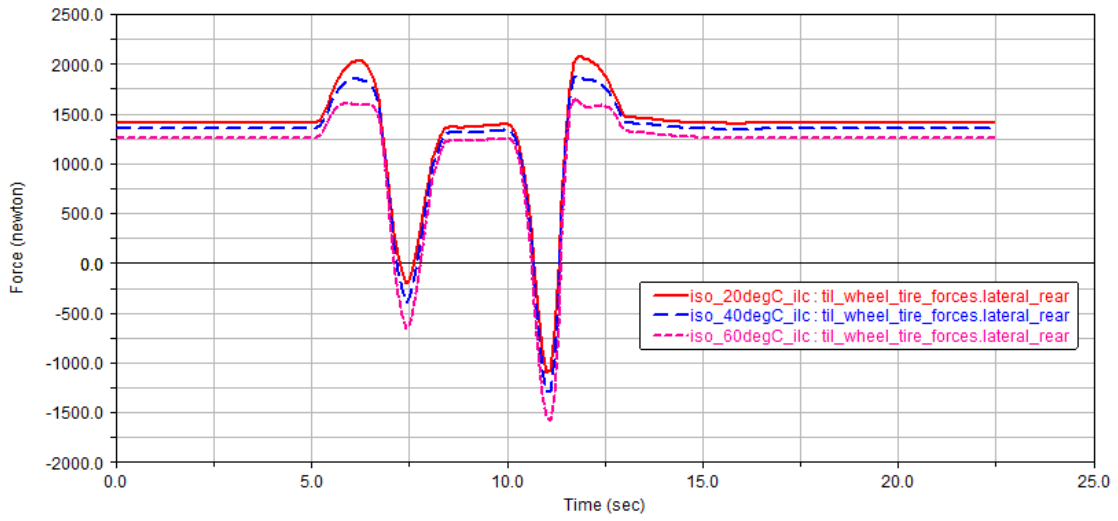


Figure 4.5: Transient response of Lateral Force at different Temperatures for Double ISO Lane Change Maneuver.

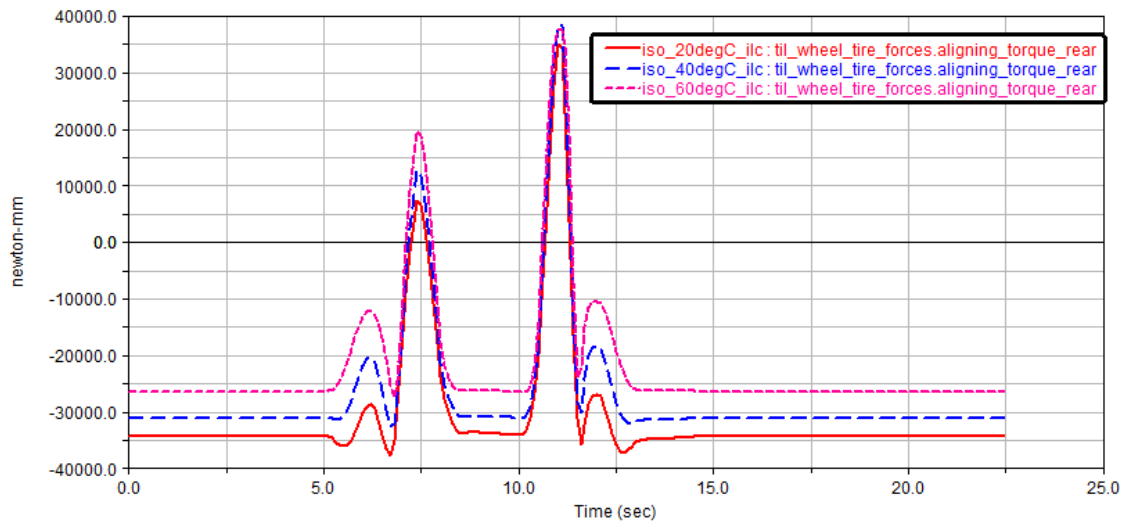


Figure 4.6: Transient response of Self Aligning Torque at different Temperatures for Double ISO Lane Change Maneuver.

4.1.2 Acceleration and Braking Analysis

To study the the transient variation of longitudinal forces with respect to slip ratio, we do the acceleration and braking Analysis. As explained in the previous section, the steady state tire models at three different temperatures are incorporated in the ADAMS car to do the the transient analysis at three different temperatures(20°C, 40°C and 60°C).

Acceleration

In order to give an acceleration maneuver, we incorporate the steady state tire model at a particular temperature to the ADAMS car and will do the simulation. This process is repeated for the the three temperatures. The acceleration is given for a duration of 15 seconds. The throttling is given at time $t=1$ sec starting from zero to a final throttle of 100 percentage at time $t=15$ sec. The initial velocity of the car is 10km/hr and step duration is unity. Figure 4.7 shows the effect of temperature on the longitudinal forces. From the graph it can be seen that when temperature increases, the longitudinal force decreases after a particular time. After a certain time the longitudinal force decreases suddenly which means that the longitudinal slip increases spontaneously. So it is clear that at this particular time the tire starts slipping without rolling. So when the temperature is increased, the vehicle/tire slips at a time earlier than at lower temperature and also peak value attained at lower temperature is more than at higher temperature. This phenomenon occurs primarily due to the decrease in friction with the increase in temperature.

Braking

Braking analysis also gives the transient response of longitudinal force w.r.t longitudinal slip ratio. We will do simulations at three different temperatures of 20°C, 40°C and 60°C by importing the steady state tire models(tire property files) at three different temperatures on the demo car in ADAMS. The braking analysis is done on a vehicle moving with initial velocity of 50km/hr. The gear is kept constant at third position and 100 percent brake is applied. Simulation is done for a time period of 10 seconds with 100 steps. Figure 4.8 shows the variation of longitudinal forces at different temperatures. It can be seen from the graph that when temperature increases, the peak value of longitudinal force decreases. Also it can be seen that the time taken by the vehicle to stop at higher temperature is more than the lower

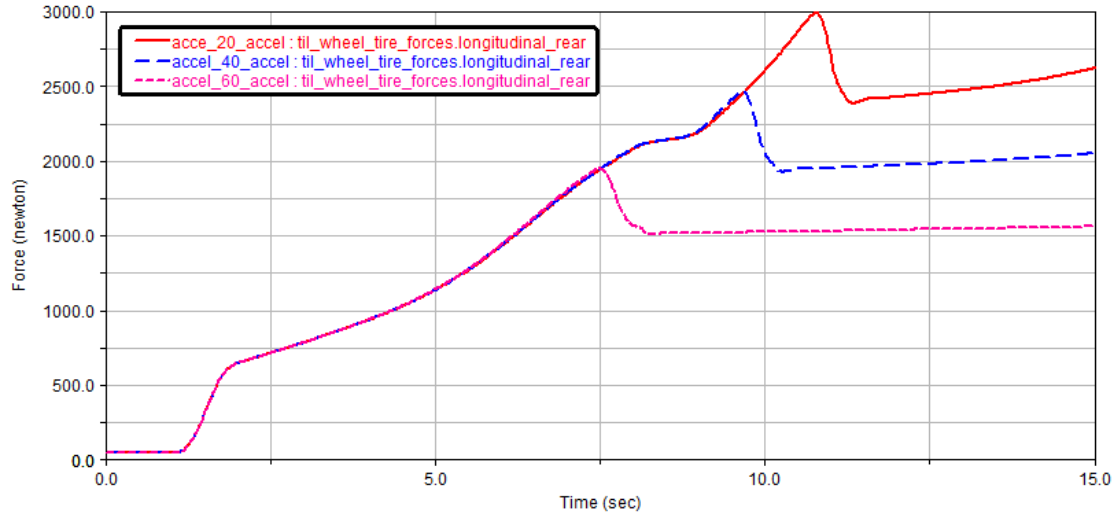


Figure 4.7: Transient response of Longitudinal Force at different Temperatures during acceleration.

temperature. For a particular temperature, after a particular time, the tire starts slipping which is shown as horizontal lines in the graph. The time at which the tire starts slipping will also be greater at higher temperature. This is because as temperature increases, the coefficient of friction decreases and hence the shear force also decreases and the vehicle starts slipping. Thus, at higher temperature, braking decreases stability.

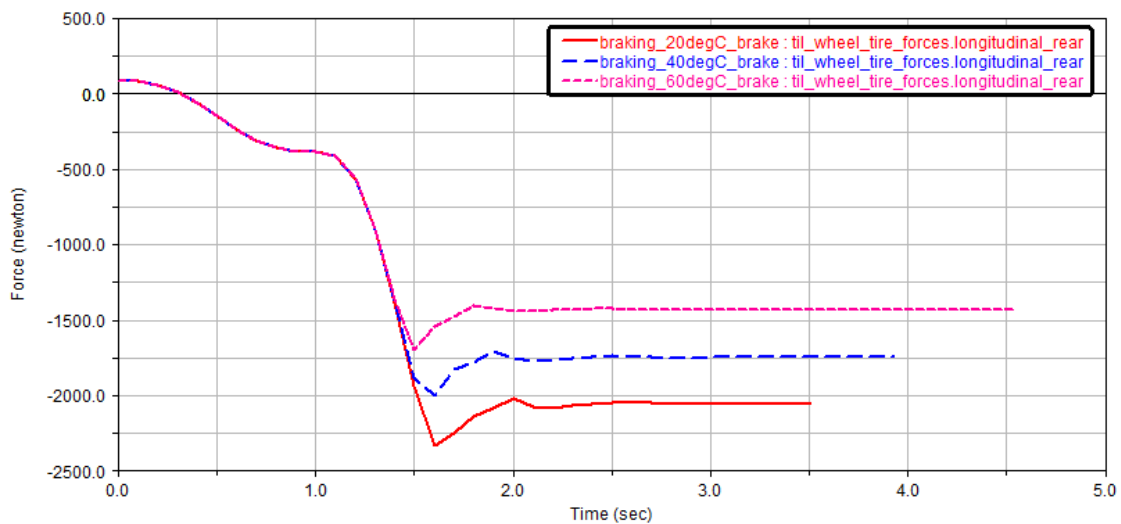


Figure 4.8: Transient response of Longitudinal Force at different Temperatures during braking.

4.2 Summary

In this chapter we have done the transient analysis of tire force and moments using MSC ADAMS, a multibody dynamics simulation software. We have imported the parameter values of modified PAC2002 models corresponding to three temperature to form three steady state tire models in ADAMS. Then we have done the steady state analysis in ADAMS and validated with FEM results at different temperatures. Then these tire models called as tire property files are replaced on an ADAMS demo car and studied the transient response of lateral force, longitudinal force and self aligning moment under going different driving maneuvers as lane change, acceleration and braking.

Chapter 5

Conclusion and Future Work

In this thesis we have studied the steady state and transient response of longitudinal force, lateral force and self aligning moment under the influence of temperature. In chapter 1 we have discussed the tire structure, tire markings, different types of tire models, different forces and moments acting on the tire-road interaction and the studies conducted by researchers on the tire characteristics. We have also discussed the experimental results on a sample piece of tire rubber conducted in the past, considering the temperature effect which we have utilized in this thesis. In chapter 2 we have discussed the magic formula based PAC2002 tire model and the modification done on the same model to include the temperature effects. Then we did the finite element modeling and analysis of a tire under steady state condition by including the effect of temperature in chapter 3. After validating the FEM results on lateral force with the experimental results by Mazahiko et. al., we have compared the steady state forces and moments from ABAQUS at different temperatures with the modified PAC2002 model and extracted the parameters. Subsequently in chapter 4 we have used these parameters to form three different steady state tire model at three different temperatures in ADAMS. The steady state analysis results from ADAMS is validated with results that we got from modified PAC2002 model in the previous chapter. After validation these tire models were used to do the transient analysis in ADAMS to study the temperature effect on the transient response of the forces and moments. We have modified the PAC2002 model to incorporate the temperature effects on longitudinal forces and lateral forces. We did the Steady State FEM Analysis by considering the variation of viscoelastic modulus with respect to temperature and variation of coefficient of friction with respect to slip speeds and temperatures. The transient analysis of the forces and moments with the effect of

temperature is done in MSC ADAMS at different maneuvers of acceleration, braking and Double Iso Lane Change.

From the analysis results of this thesis, it can be seen that when the temperature increases the tire forces and moments decreases, which will lead to the instability of the vehicle, both in lateral and longitudinal direction. This thesis can be continued by the validation of the steady state results and transient response with the experimental results at different temperatures. We have employed a hybrid approach to do the steady state analysis in ABAQUS. But we can incorporate the governing equations by incorporating temperature effects in ABAQUS using FORTRAN. We can use the same approach to study the tire characteristics at higher temperatures, by conducting experiments on a sample piece of tire rubber at higher temperatures. From the thesis, it is clear that increase in temperature causes less traction and decrease in directional stability.

References

- [1] Teaching; Desertations <http://www.multibody.net/teaching/dissertations/2011-tomasi>, 2011
- [2] Thomson, J., What we should know about tires, *Internet* , <http://www.jags.org/TechInfo/2001/05May/tires> , 2003.
- [3] Pacejka. H. B, Tire and Vehicle Dynamics, *New York: Elsevier*, 2012
- [4] Jazar R. N., Vehicle dynamics: Theory and application, *New York: Springer*. 2008
- [5] H. Pacejka, Modeling of the Pneumatic Tyre and its Impact on Vehicle Dynamic Behavior, *Delft* , 1988
- [6] Gipser M., FTire, a New Fast Tire Model for Ride Comfort Simulations, *International ADAMS User's Conference Berlin, Germany* , 1999.
- [7] Loo, M. A Model Analysis of Tire behavior Under Vertical Loading and Straight Line Free Rolling, *Tire Science and Technology*, **13(2)**, 67-90, 1985.
- [8] Davis D. C, A Radial-Spring Terrain-Enveloping Tire Model, *Vehicle System Dynamics*, **3**, 1974.
- [9] Allen, R. W., Magdaleno, R. E., Rosenthal, T. J., Klyde, D. H., Hogue, J. R, Tire Modeling Requirements for Vehicle Dynamic Simulation, *Society of Automobile Engineers*, SAE Paper 950312, 1995.
- [10] Rotta, J. Zur Statik des Luftreifens, *Ingenieur-Archiv*, **17**, 129-141, 1949
- [11] Rhyne, T.B., Cron, S.M., Development of a non-pneumatic wheel, *Tire Sci. Technol*, **34**, 150-169, 2006.

- [12] Dunn, S.E. and Zorowski, C.F., A study of internal stresses in statically deformed pneumatic tires, *Office of Vehicle Systems Research Contract CST-376, US National Bureau of Standards, Washington, D.C.*, 1970
- [13] Ridha, R.A., Satyamurthy, K. and Hirschfeld, L.R., Finite element modeling of a homogeneous pneumatic tire subjected to footprint loadings, *Tire Sci. Technol* **13** (2), 91-110, 1985
- [14] Chang, J.P., Satyamurthy, K. and Tseng, N.T., An efficient approach for the three-dimensional finite element analysis of tires, *Tire Sci. Technol* **16** (4), 249-273), 1988
- [15] L. O. Faria, J. T. Oden, B. Yavari, W. W. Tworzydło, J. M. Bass, and E. B. Becker, Tire modeling by finite elements. Tire Sci. Technology, *Tire Sci. Technology*. **20**(1), 33–56, 1992.
- [16] K.T. Danielson, A.K. Noor, Finite elements developed in cylindrical coordinates for three-dimensional tire analysis, *Tire Sci. Technol* **25** (1), 2–28, 1997
- [17] Luchini, J.R. and Popio, J.A., Modeling transient rolling resistance of tires, *Tire Sci. Technol* **35** (2), 118-140, 2007
- [18] J.R. Cho, H.W. Lee, W.B. Jeong, K.M. Jeong, K.W. Kim, Numerical estimation of rolling resistance and temperature distribution of 3-D periodic patterned tire, *International Journal of Solids and Structures* **50**, 86–96, 2013
- [19] Tian Tang, Daniel Johnson, Emily Ledbury, Thomas Goddette, Sergio D. Felicelli, Robert E. Smith, Simulation Of Thermal Signature Of Tires and Tracks, *Ground Vehicle Systems Engineering and Technology Symposium (GVSETS)* 2012
- [20] Daniel D. Higgins, Brett A. Marmo, Christopher E. Jeffree, Vasileios Koutsos, Jane R. Blackford, Morphology of ice wear from rubber–ice friction tests and its dependence on temperature and sliding velocity, *Wear* **175**, 634-644, 2008
- [21] Kevin Menard, Dynamic Mechanical Analysis: A Practical Introduction, 2nd Edition, *CRC Press* 2008
- [22] B N J Persson, Rubber friction: role of the flash temperature, *Journal of Physics: Condensed Matter* **18**, 7789–7823, 2006

- [23] Korunovic, N., Trajanivic, M., Stojkovic, M., Mistic, D. and Milovanovic, J. Finite Element Analysis of a Tire Steady Rolling on the Drum and Comparison with Experiment. *Journal of Mechanical Engineering*, **57 (12)** , 888-897, 2011.
- [24] Bibin S, Atul Gavade, Ashok Kumar Panday, Dynamic Analysis of Tire Forces and Moment Using Hybrid Approach, *The 22nd International Congress of Sound and Vibration* 2015
- [25] Masahiko Mizuno, Hideki Sakai, Kozo Oyama, Yoshitaka Isomura, The Development of the Tire Side Force Model Considering the dependence of Surface temperature of the Tire, *Vehicle Systems Dynamics Supplement : Taylor and Francis Ltd* **41**, 361-370, 2004
- [26] Reference manual, *ABAQUS 6.9*, [Online.] available: <http://www.3ds.com/products-services/simulia/portfolio/abaqus>, 2012.
- [27] Atul Gavade, Analysis and Comparison of Different Tire Models under Riding and Turning Conditions, *Master of Technology Thesis, Post Graduate Program in Mechanical and Aerospace Engineering, IIT Hyderabad*, 2014.
- [28] Reference manual, *MSC ADAMS*, [Online.] available: <http://www.mscsoftware.com/product/adams>, 2011.